Published in final edited form as:
Biochem J. 2014 April 15; 459(2): 417–425. doi:10.1042/BJ20131037.

S-palmitoylation regulates biogenesis of core glycosylated wild-type and F508del CFTR in a post-ER compartment

M.L. McClure[*,†], **H. Wen**[*], **J. Fortenberry**[*], **J.S. Hong**[*,‡], and **E.J. Sorscher**[*,§,1]

[*]Gregory Fleming James Cystic Fibrosis Research Center, University of Alabama at Birmingham, Birmingham, AL 35294, USA

[†]Department of Genetics, University of Alabama at Birmingham, Birmingham, AL 35294, USA

[‡]Department of Cell, Developmental and Integrative Biology, University of Alabama at Birmingham, Birmingham, AL 35294, USA

[§]Department of Medicine, University of Alabama at Birmingham, Birmingham, AL 35294, USA

Abstract

Defects in CFTR maturation are central to the pathogenesis of cystic fibrosis (CF). Palmitoylation serves as a key regulator of maturational processing in other integral membrane proteins, but has not been tested previously for functional effects on CFTR. In this study, we used metabolic labeling to confirm that wild-type and F508del CFTR are palmitoylated, and show that blocking palmitoylation with the pharmacologic inhibitor 2-bromopalmitate (2-BP) decreases steady state levels of both wild-type and low temperature-corrected F508del CFTR, disrupts post-ER maturation, and reduces ion channel function at the cell surface. Protein acyl transferases (PATs) comprise a family of 23 gene products that contain a DHHC motif and mediate palmitoylation. Recombinant expression of specific PATs led to increased levels of CFTR protein and enhanced palmitoylation as judged by western blot and metabolic labeling. Specifically, we show that DHHC-7: 1) increases steady state levels of wild-type and F508del CFTR band B, 2) interacts preferentially with the band B glycoform, and 3) augments radiolabeling by ^{3}H-palmitic acid. Interestingly, immunofluorescence revealed that DHHC-7 also sequesters the F508del protein to a post-ER (Golgi) compartment. Our findings point to the importance of palmitoylation during wild-type and F508del CFTR trafficking.

Keywords

palmitoylation; post-translational modification; protein trafficking; protein maturation; cystic fibrosis

[1]To whom correspondence should be addressed. sorscher@uab.edu..

AUTHOR CONTRIBUTION Michelle L. McClure, Jeong S. Hong, and Eric J. Sorscher designed the research. Michelle L. McClure and Jeong S. Hong performed experiments and analyzed data. James Fortenberry collected data in Figure S1. Hui Wen prepared DNA and specific reagents. Michelle L. McClure and Eric J. Sorscher wrote the paper.

INTRODUCTION

Cystic fibrosis is a disease caused by mutations of the cystic fibrosis transmembrane conductance regulator (CFTR), an ion channel responsible for transport of chloride and bicarbonate. Expression of CFTR is critical for proper function of numerous exocrine tissues including the lungs, intestinal tract, pancreas, liver, sweat glands, and vas deferens. The most common disease-causing mutation is deletion of phenylalanine at position 508 (F508del) which contributes to upwards of 90% of clinical CF in the United States and Europe. Wild-type CFTR undergoes core-*N*-glycosylation in the endoplasmic reticulum (ER) and is further processed by the Golgi apparatus where complex glycan attachment occurs. Following trafficking to the plasma membrane, the fully glycosylated channel protein is internalized by early endosomes and subsequently recycled to the cell surface or targeted for lysosomal proteolysis (1, 2). F508del CFTR is recognized as misfolded in the ER and sequestered for ER-associated degradation (ERAD) via the ubiquitin-proteasome system (UPS) (2–4). This processing defect is partially overcome by growth of epithelial cells at low temperature (~27°C) or treatment with small molecule correctors that result in F508del CFTR surface localization. Misfolded CFTR that escapes ERAD and traffics to the cell surface retains partial function as an ion transporter, although the protein is rapidly internalized and marked by ubiquitin for degradation, resulting in a decreased peripheral half-life (2, 5–7).

Covalent modifications such as glycosylation and phosphorylation are crucial for proper biogenesis and function of membrane proteins such as CFTR. For example, *N*-glycosylation increases the surface stability of CFTR by blunting internalization (1, 8). CFTR channel gating utilizes PKA-dependent phosphorylation to promote NBD1–NBD2 (nucleotide binding domain) heterodimerization followed by ATP binding and hydrolysis at the dimer interface (9–12). On the other hand, phosphorylation at specific serines in the CFTR regulatory domain (RD) inhibits channel activity, and substitution of these residues by alanine increases channel conductance (13). CFTR covalent modifications may also have therapeutic significance. For example, small molecule potentiators have been identified that augment mutant CFTR activity by enhancing phosphorylation of the regulatory domain (14).

Using mass spectrometry, we recently identified a novel CFTR post-translational modification (PTM), S-palmitoylation (15). The PTM is characterized by covalent attachment of palmitate, a 16-carbon saturated fatty acid, to cysteine residues via thioester linkage on sulfhydryl groups. Unlike other types of lipidation, thioester-linked palmitate modification is rapidly reversible, allowing proteins to undergo regulated cycles of S-palmitoylation and depalmitoylation (16, 17). For soluble substrates, attachment of palmitate typically promotes membrane association and often occurs in conjunction with *N*-myristoylation or prenylation. Palmitoylation of membrane proteins regulates protein-protein interaction by altering transmembrane orientation (18–20), controls other side chain attachments (18, 20–22), or serves as a signal for sorting to various cellular compartments (23–25). In particular, protein localization, maturational processing, and function of numerous ion channels and ABC transporters are believed to be regulated in this fashion. For example, palmitoylation has been implicated during protein insertion into the plasma membrane (GluR1 subunit of AMPAR; (18)), recycling from the cell surface (MUC1; (26)),

ion channel phosphorylation (ENaC; (27)), channel gating (BK potassium channels; (21)), and transporter function of peptides closely related to CFTR (ABCA1; (28)). Notably, many of these processes closely parallel those disrupted by F508del.

Our earlier studies (15) provided evidence for CFTR palmitoylation but did not address the functional or biochemical significance of this modification. Based on the emerging appreciation of palmitoylation as a key regulator of membrane protein maturation and a molecular target in other diseases of peptide folding (29–33), the present experiments were intended to build upon our previous findings (15) and address the following questions. First, does palmitoylation participate in CFTR biogenesis, and does blocking this pathway influence surface ion transport? Second, is F508del CFTR palmitoylated, and is rescue of the mutant protein altered by this modification? Third, can we define specific molecular mechanisms that underlie CFTR palmitoylation, and are there cellular acyl transferase enzymes that bind CFTR and modulate palmitate side chain attachment? We show that treatment of F508del CFTR with one such enzyme (DHHC-7) leads to increased core glycosylated (band B) CFTR and sequesters the protein in a post-ER (Golgi) compartment. The findings establish an important role for palmitoylation during CFTR biogenesis and rescue of the F508del mutant.

EXPERIMENTAL

Cell models and reagents

HeLa CCL2 and HEK293 cells were purchased from ATCC (Manassas, VA). Stably transduced HeLa cells (expressing wild-type or F508del CFTR) were a gift of Dr. J. Kappes (University of Alabama at Birmingham) (34). All cells were cultured in Dulbecco's modified eagle medium (DMEM; Invitrogen, Carlsbad, CA) supplemented with 10% fetal bovine serum (FBS). Transfections were performed using *Trans*IT®-LT1 or *Trans*IT-HeLaMONSTER® reagents (Mirus Bio, Madison, WI) per manufacturer instructions. CFTR-specific antibodies included: 10B6.2 – anti-human NBD1 monoclonal antibody (produced in mouse); 24–1 – anti-C-terminus monoclonal antibody (produced in mouse); and 3G11 – anti-NBD1 monoclonal antibody (produced in rat) (CFTRfolding.org).

Palmitate side chain labeling

Cells were grown in 6-well or 10 cm plates. Prior to study, tissue culture medium was replaced with DMEM supplemented with 2% dialyzed FBS and 1% non-essential amino acids for 1 h at 37°C. Following serum deprivation, cells were labeled with 500 μCi/ml ^{3}H-palmitic acid (PerkinElmer, Waltham, MA) for 4 h in DMEM as above, rinsed, and collected in cold PBS with lysis in RIPA buffer. CFTR was immunoprecipitated using 24–1 or 10B6.2 antibody conjugated to protein A/G agarose (Thermo Scientific Pierce Protein Biology Products, Rockford, IL), followed with rinsing and release by 37°C incubation in 4X Laemmli sample buffer containing 10% β-mercaptoethanol. Protein was separated by SDS-PAGE (6% acrylamide) and CFTR detected using autoradiography (Biomax MR film (Kodak) for 3–6 months though a Kodak Biomax transcreen-LE intensifying screen at −80°C). Quantitation was performed with ImageLab software (Bio-Rad Laboratories, Hercules, CA).

Western blot analysis

Cells were washed with PBS and lysed with Triton X-100 buffer containing 1X protease inhibitor cocktail and EDTA for 45 min on ice. Following centrifugation, pellets were discarded and protein concentration measured using BCA protein assay (Thermo Scientific Pierce). Equal amounts of protein (15–30 μg) were incubated in 4X Laemmli buffer with 10% β-mercaptoethanol at 37°C for 15 min, electrophoresed though a 6% or 4–12% SDS-PAGE gel, and transferred to PVDF membrane. Blocking was in 1X PBS, 0.1% Tween-20, and 5% non-fat dehydrated milk for 30 min at room temperature followed by overnight incubation at 4°C with the indicated primary antibody in blocking buffer. After thee washes (1X PBS + 0.1% Tween-20), membranes were incubated with secondary antibody conjugated to horseradish peroxidase followed by chemiluminescence with SuperSignal West Femto or West Pico Chemiluminescent Substrate (Thermo Scientific Pierce). Membranes were imaged using ChemiDoc XRS HQ (Bio-Rad) or Kodak Biomax MR film. Densitometry was performed with Quantity One or ImageLab software (Bio-Rad).

Co-immunoprecipitation

Cells transfected with HA-conjugated DHHC proteins (gift of the Fukata laboratory, National Institute for Physiological Sciences, Okazaki, Japan) were grown to 90% confluence in 6-well plates and collected by scraping into cold PBS. Following lysis with Triton X-100 buffer and immunoprecipitation using mouse anti-HA antibody conjugated to protein A/G agarose (Thermo Scientific Pierce), protein-agarose mixtures were separated by 6% SDS-PAGE. CFTR was detected by western blot with rat 3G11 monoclonal antibody. Densitometry was conducted as above.

Pulse-chase

Cells were grown to ~80% confluence in 6-well plates. Prior to labeling, tissue culture medium was replaced with methionine-cysteine-free DMEM supplemented with 1% non-essential amino acids for 1 h at 37°C. After methionine-cysteine starvation, cells were pulse labeled with 150 μCi/ml EasyTag™ EXPRESS^{35}S Protein Labeling Mix (PerkinElmer) for 30 min in methionine-cysteine-free DMEM supplemented with 1% non-essential amino acids. Radioactive medium was exchanged with complete medium and cultured for various chase periods with or without the palmitoylation inhibitor 2-bromopalmitate (2-BP, 100 μM, Sigma Aldrich, St. Louis, MO). 2-BP is a blocker of palmitoylation (35–40), but also has been shown to exhibit off target effects such as inhibition of carnitine palmitoyl transferase or glucose-6-phosphatase (41, 42). Cells were lysed in RIPA buffer at the time points indicated and immunoprecipitated using 24–1 antibody conjugated to protein A/G agarose. Following pull-down, protein-agarose mixtures were prepared and separated as above by SDS-PAGE and CFTR detected by autoradiography. Maturation efficiency was measured using ImageLab by comparing density of fully glycosylated (band C) at each time point to the total (labeled) CFTR immediately following the pulse.

Halide efflux assay (SPQ)

Cells were seeded onto Vectabond®-treated glass coverslips and grown to ~80% confluence. Immediately prior to study, hypotonic loading of cells was accomplished with

the halide quenched dye 6-methoxy-*N*-(3-sulfopropyl)quinolinium (SPQ, 10 mM, Molecular Probes Inc., Eugene, OR) for 10 min followed by incubation with quenching NaI-based buffer (43). CFTR robustly conducts iodide in addition to chloride, HCO_3^-, and other anions, allowing use of iodide quench as a measure of macroscopic channel activity. Cells were mounted in a specially designed perfusion chamber and fluorescence monitored using an inverted Nikon Diaphot microscope (Tokyo, Japan; excitation at 350 nm, emission at >410 nm), an Easy Ratio Pro imaging system (PTI, Birmingham, NJ), and a CoolSNAP HQ_2 camera (Photometrics, Tucson, AZ). Baseline fluorescence was initially studied in NaI buffer (above) followed by dequenching $NaNO_3$ solution (43). CFTR agonists (20 μM forskolin, 50 μM genistein) were added to activate channel gating, after which NaI buffer was again perfused. Fluorescence was normalized for each cell versus baseline and increases shown as percent above basal (quenched) values. Approximately 30 individual cells were monitored per coverslip. Averages from each coverslip were used for statistical analysis (n = 5–6 coverslips per condition).

Short-circuit current measurements

Inserts were mounted in Ussing chambers and Isc tested under voltage clamp conditions as previously described (44). Briefly, Calu-3 or CFBE cells expressing wild-type CFTR were seeded on permeable supports (5×10^5 cells/filter, 6.5 mm diameter) coated with fibronectin. Cells were grown to confluence followed by propagation at air-liquid interface. Filters in modified Ussing chambers (Jim's Instruments, Iowa City, IA) were bathed on both sides with identical Ringers buffer containing 120 mM NaCl, 25 mM $NaHCO_3$, 2.4 mM KH_2PO_4, 1.24 mM K_2HPO_4, 1.2 mM $CaCl_2$, 1.2 mM $MgCl_2$, 10 mM D-glucose (pH 7.4). Bath solutions were vigorously stirred and gassed with 95% O_2:5% CO_2 and maintained at 37°C. Short-circuit current (Isc) was monitored using an epithelial voltage clamp (University of Iowa Bioengineering, Iowa City, IA). A 3-mV pulse of 1 second duration was imposed every 100 seconds to track resistance by Ohm's law. To measure stimulated Isc, the mucosal bathing solution was changed to a low Cl^- buffer containing 1.2 mM NaCl, 115 mM Na gluconate, and other components as above plus 100 μM amiloride to block residual Na^+ channel activity. Agonists (20 μM forskolin and 50 μM genistein) were included in the bath solutions (minimum 5 min observation at each concentration). $CFTR_{Inh}$-172 (10 μM) was added to the mucosal bathing solution at the conclusion of each experiment to block CFTR-dependent Isc.

Immunofluorescence

HeLa cells stably transduced with wild-type or F508del CFTR were grown on Vectabond®-treated glass coverslips. Approximately 48 h following transfection with HA-tagged DHHC-7 or empty vector, cells were rinsed with PBS, fixed with 4% paraformaldehyde in 1X PBS at room temperature for 20 min, and rinsed again with PBS. After permeabilization and blocking in 1X PBS with 10 mg/ml BSA and 0.1% Triton X-100 (30 min), cells were labeled with rat 3G11 and/or mouse anti-HA antibodies (1:2000) for 2 h in 1X PBS containing 10 mg/ml BSA and 0.1% Triton X-100. Cells were then fluorescently probed with anti-rat IgG Alexa Fluor 647 and/or anti-mouse IgG Alexa Fluor 555 antibodies (1:2000; Life Technologies, Grand Island, NY) for 1 h in 1X PBS containing 10 mg/ml BSA and 0.1% Triton X-100. Samples were labeled with Hoechst nuclear stain (Life

Technologies), rinsed thoroughly with PBS, mounted onto glass slides, and stored at 4°C. Imaging was conducted with a Zeiss LSM 710 confocal laser scanning microscope (Oberkochen, German).

Statistics

Data were expressed as mean ± SEM and tested for significance using paired or unpaired Student's *t* test. Results with $P < 0.05$ were considered significant.

RESULTS

CFTR is modified by S-palmitoylation

CFTR palmitoylation was demonstrated by metabolically labeling HeLa cells with ^{3}H-palmitic acid (Figure 1A). Following immunoprecipitation with an anti-NBD1 antibody, autoradiography indicated that both mature, fully glycosylated (band C) and immature, ER-localized (band B) wild-type CFTR glycoforms are palmitoylated. F508del CFTR (band B) is also palmitoylated, and cells grown at 27°C (to partially rescue the F508del maturational defect) demonstrate palmitate-labeling of bands B and C (Figure 1A). As a control, cells were treated with 2-bromopalmitate (2-BP), a pharmacologic inhibitor of palmitoylation. 2-BP binds irreversibly to coenzyme A, a primary step in the palmitoylation pathway, thereby preventing palmitate side chain attachment (35, 41). ^{3}H-palmitate labeling was strongly diminished following treatment of cells with 2-BP (Figure 1B).

Palmitoylation is required for proper trafficking of wild-type CFTR

CFTR expression was examined by western blot analysis following metabolic treatment with 2-BP. In order to demonstrate cell line independence, we tested HeLa cells stably transduced to express wild-type CFTR, CFBE (cystic fibrosis bronchial epithelial) cells stably expressing wild-type CFTR, Calu-3 cells (pulmonary epithelial cells that express CFTR from the endogenous promoter), and HEK293 cells encoding doxycycline-inducible CFTR. In all cases, general disruption of palmitoylation in cells led to diminished levels of steady state CFTR, suggesting a role during protein biogenesis. To specifically test the importance of palmitoylation during CFTR maturation, progression of band B to the band C glycoform was tracked via metabolic labeling and pulse-chase. Disruption of palmitoylation by 2-BP was found to impair CFTR trafficking (Figure 2 B and C).

CFTR function at the cell surface was investigated using the fluorescent indicator 6-methoxy-*N*-(3-sulfopropyl)quinolinium (SPQ), with channel activity monitored following cAMP-dependent activation. Total surface activity levels of low temperature corrected F508del were significantly decreased when palmitoylation was inhibited with 2-BP (Figure 2 D and E), a result consistent with reduced expression of mature CFTR observed by western blot and pulse-chase. Similar results were observed when short circuit currents were monitored in CFBE and Calu-3 monolayers by Ussing chamber analysis (Figure S1).

Palmitoylation contributes to rescue of the F508del CFTR biogenesis defect

Deletion of phenylalanine 508 leads to misfolded CFTR that is prematurely targeted for ERAD and does not properly traffic to the cell surface. Cell growth at low temperature

(27°C) partially corrects this defect, as evidenced by the increase in band C expression. However, F508del rescue by low temperature is impaired in cells treated with 2-BP (Figure 3A), suggesting that palmitate attachment is important for ER to plasma membrane rescue of the mutant protein. Concordant with this data, surface activity levels of low temperature corrected F508del CFTR were significantly decreased when palmitoylation was inhibited by 2-BP (Figure 3 B and C).

Multiple PATs regulate wild-type and F508del CFTR expression

Palmitoylation of target proteins is mediated by protein acyl transferase (PAT) enzymes, whereas palmitate removal is carried out by acyl thioesterases. To date, twenty-three mammalian PATs have been identified, all of which contain a DHHC zinc finger domain (PATs are therefore also termed `DHHC' proteins) (38). We tested the twenty-three DHHC enzymes (gift of the Fukata laboratory, National Institute for Physiological Sciences, Okazaki, Japan) for effects on CFTR protein. In cells expressing wild-type CFTR, specific DHHCs strongly influence the immature glycoform. In particular, DHHC-3 and DHHC-7 led to a robust increase of band B CFTR (Figure 4A). Co-immunoprecipitation indicated a binding interaction between DHHC-7 (or to lesser extent DHHC-3) and band B, while DHHC-6, for example, showed no interaction (Figure 4C). Similarly, co-transfection of DHHC-7 with F508del CFTR increased steady state levels of the mutant protein (Figure 4B), and co-immunoprecipitation again indicated a clear interaction (Figure 4D). Notably, DHHC-3 and DHHC-7 are structurally related and known to exhibit similar spectrum of activity in other palmitoylated proteins (45, 46).

Since DHHC-7 exhibited the strongest effects on both wild-type and F508del CFTR, we next determined whether the enzyme specifically alters CFTR palmitoylation. Cells were co-transfected with HA-tagged CFTR and HA-tagged DHHC-7, followed by metabolic labeling with ^{3}H-palmitic acid. CFTR was pulled down using an anti-HA antibody and exposed on film for a time interval considerably shorter than that required to detect tritium labeling of CFTR without DHHC transfection (i.e. 3–4 weeks versus several months). DHHC-7 expression led to a strong and readily detectable signal after a short (3–4 week) exposure, suggesting an increase in CFTR palmitoylation (Figure 4E).

DHHC-7 palmitoylates and increases the level of F508del and wild-type CFTR in the Golgi

Since DHHC-7 co-immunoprecipitates strongly with both wild-type and F508del CFTR, we investigated the compartment in which this interaction occurs. Cells expressing F508del or wild-type CFTR were transfected with HA-tagged DHHC-7 or empty vector, labeled with anti-CFTR or anti-HA antibody, and followed by fluorophore-tagged secondary antibody. Under basal conditions (empty vector transfection), F508del CFTR expression is barely detectable (Figure 5, column I); however F508del levels are significantly increased when DHHC-7 is overexpressed (Figure 5, column II). Both F508del and wild-type CFTR were found to strongly co-localize with DHHC-7, primarily with Golgi markers (Figures 5 and S2, columns II–IV). This finding is consistent with previous studies indicating that DHHC-7 is present in the Golgi and plasma membrane but not ER (39, 47–49). The localization of F508del CFTR was unexpected and indicates sequestration of the mutant protein to a post-ER compartment.

DISCUSSION

Palmitate attachment has been shown previously to serve as a regulator of cell surface targeting, protein trafficking, and stability (18, 20, 22–26). For example, H-Ras is palmitoylated at cysteine residues that mediate a reversible palmitoylation-depalmitoylation step and control partitioning between the Golgi and plasma membrane (50). In MUC1 and the GABAA receptor, protein turnover and half-life are palmitoylation dependent (26, 51). For other transmembrane proteins, including certain voltage sensitive ion channels, palmitoylation is the key determinant of membrane localization (40). Findings described in the present study establish that both wild-type and F508del CFTR serve as substrates for palmitoylation, and blocking this mechanism in cells interferes with normal CFTR biogenesis.

Metabolic labeling was used to confirm palmitoylation of wild-type and F508del CFTR (Figure 1A). Treatment with 2-BP, a pharmacologic inhibitor of palmitoylation, resulted in decreased steady state levels and activity of the wild-type protein, as well as diminished palmitate side chain attachment (Figure 1 and 2). In the setting of low-temperature correction, F508del band C was also significantly diminished (Figure 3). Our data therefore suggest a previously unrecognized role for palmitoylation during CFTR maturation. We also investigated effects of the twenty-three known mammalian protein acyl transferases on CFTR modulation and identified DHHC-7 as a robust enhancer of both wild-type and F508del CFTR band B (Figure 4). This effect involves an interaction (direct or indirect) between CFTR and DHHC-7 (Figure 4 C and D), occurs predominantly in the Golgi (Figure 5), and is concordant with previous reports indicating DHHC-7 localization to post-ER compartments (39, 47–49). Small amounts of F508del CFTR have been shown previously to traffic beyond the ER *in vitro* and *in vivo*, and low levels of the mutant protein are believed to escape ERAD and arrive in functional form at the plasma membrane (52–55). We therefore favor an interpretation in which covalent attachment of palmitate sequesters wild-type and F508del CFTR in the early Golgi, leading to accumulation of an immature glycoform (Figure 4, Figure 5, and Figure S2). The observations that 1) 2-BP blocks CFTR biogenesis, and 2) palmitoylated CFTR accumulates in the Golgi suggests that another event (e.g. removal of the attached palmitate group via thioesterase modification) is required for further maturation and subsequent glycan attachment. Such a mechanism has been shown previously to regulate BK channel exit from the *trans*-Golgi network, leading to cell surface expression (40). Additional studies will be necessary to determine whether the increased pool of band B attributable to DHHC-7 is “correctable” by F508del rescue strategies, a result that would suggest a role for these enzymes as molecular targets in cystic fibrosis.

Covalent attachment of palmitate contributes to pathogenesis in diseases such as Huntington's, neuronal ceroid lipofuscinosis, and X-linked mental retardation (29–32). Cell-specific palmitoylomes (e.g. from epithelial and other cell types (56–59)) have been applied as means to expand understanding of both protein trafficking and disease mechanism, and point to the importance of investigating this modification in airway epithelial tissues. Although palmitoylation is a seminal post-translational regulator of protein biogenesis, its role during CFTR maturation has not been reported previously. New methods for CFTR purification (15), together with increasingly sensitive techniques such as acyl biotin

exchange (60) are being used by our laboratory to investigate specific palmitoylated residues in wild-type and F508del CFTR. The present results furnish a means by which the role of palmitoylation, including its contribution to F508del processing, can be more fully understood in the future.

Supplementary Material

Refer to Web version on PubMed Central for supplementary material.

Acknowledgments

We thank Masaki Fukata (National Institute for Physiological Sciences, Okazaki, Japan Fukata) for the generous gift of the DHHC library used in our protein acyl transferase studies. We also thank the laboratory of John C. Kappes for providing the modified HeLa, CFBE, and HEK293 cell lines. Special thanks to Shawn Williams for assisting with the immunofluorescence analysis.

FUNDING This work was supported by the Cystic Fibrosis Foundation [R464-CR11, SORSCH05XXO] and the National Institutes of Health [P30 DK072482].

Abbreviations used

2-BP	2-bromopalmitate
CF	cystic fibrosis
CFBE	cystic fibrosis bronchial epithelium
CFTR	cystic fibrosis transmembrane conductance regulator
DMEM	Dulbecco's modified eagle medium
ER	endoplasmic reticulum
ERAD	ER-associated degradation
FBS	fetal bovine serum
NBD	nucleotide binding domain
PAT	protein acyl transferase
PTM	post-translational modification
SPQ	6-methoxy-*N*-(3-sulfopropyl)quinolinium
UPS	ubiquitin-proteasome system.

REFERENCES

1. Glozman R, Okiyoneda T, Mulvihill CM, Rini JM, Barriere H, Lukacs GL. N-glycans are direct determinants of CFTR folding and stability in secretory and endocytic membrane traffic. J. Cell. Biol. 2009; 184:847–862. [PubMed: 19307599]
2. Sharma M, Pampinella F, Nemes C, Benharouga M, So J, Du K, Bache KG, Papsin B, Zerangue N, Stenmark H, Lukacs GL. Misfolding diverts CFTR from recycling to degradation: quality control at early endosomes. J. Cell. Biol. 2004; 164:923–933. [PubMed: 15007060]
3. Ward CL, Omura S, Kopito RR. Degradation of CFTR by the ubiquitin-proteasome pathway. Cell. 1995; 83:121–127. [PubMed: 7553863]

4. Gelman MS, Kannegaard ES, Kopito RR. A principal role for the proteasome in endoplasmic reticulum-associated degradation of misfolded intracellular cystic fibrosis transmembrane conductance regulator. J. Biol. Chem. 2002; 277:11709–11714. [PubMed: 11812794]
5. Swiatecka-Urban A, Brown A, Moreau-Marquis S, Renuka J, Coutermarsh B, Barnaby R, Karlson KH, Flotte TR, Fukuda M, Langford GM, Stanton BA. The short apical membrane half-life of rescued {Delta}F508-cystic fibrosis transmembrane conductance regulator (CFTR) results from accelerated endocytosis of {Delta}F508-CFTR in polarized human airway epithelial cells. J. Biol. Chem. 2005; 280:36762–36772. [PubMed: 16131493]
6. Heda GD, Tanwani M, Marino CR. The Delta F508 mutation shortens the biochemical half-life of plasma membrane CFTR in polarized epithelial cells. Am. J. Physiol. Cell Physiol. 2001; 280:C166–174. [PubMed: 11121388]
7. Lukacs GL, Chang XB, Bear C, Kartner N, Mohamed A, Riordan JR, Grinstein S. The delta F508 mutation decreases the stability of cystic fibrosis transmembrane conductance regulator in the plasma membrane. Determination of functional half-lives on transfected cells. J. Biol. Chem. 1993; 268:21592–21598. [PubMed: 7691813]
8. Chang XB, Mengos A, Hou YX, Cui L, Jensen TJ, Aleksandrov A, Riordan JR, Gentzsch M. Role of N-linked oligosaccharides in the biosynthetic processing of the cystic fibrosis membrane conductance regulator. J. Cell Sci. 2008; 121:2814–2823. [PubMed: 18682497]
9. Mense M, Vergani P, White DM, Altberg G, Nairn AC, Gadsby DC. In vivo phosphorylation of CFTR promotes formation of a nucleotide-binding domain heterodimer. EMBO J. 2006; 25:4728–4739. [PubMed: 17036051]
10. He L, Aleksandrov AA, Serohijos AW, Hegedus T, Aleksandrov LA, Cui L, Dokholyan NV, Riordan JR. Multiple membrane-cytoplasmic domain contacts in the cystic fibrosis transmembrane conductance regulator (CFTR) mediate regulation of channel gating. J. Biol. Chem. 2008; 283:26383–26390. [PubMed: 18658148]
11. Wang W, Wu J, Bernard K, Li G, Wang G, Bevensee MO, Kirk KL. ATP-independent CFTR channel gating and allosteric modulation by phosphorylation. Proc. Natl. Acad. Sci. U. S. A. 2010; 107:3888–3893. [PubMed: 20133716]
12. Cheng SH, Rich DP, Marshall J, Gregory RJ, Welsh MJ, Smith AE. Phosphorylation of the R domain by cAMP-dependent protein kinase regulates the CFTR chloride channel. Cell. 1991; 66:1027–1036. [PubMed: 1716180]
13. Wilkinson DJ, Strong TV, Mansoura MK, Wood DL, Smith SS, Collins FS, Dawson DC. CFTR activation: additive effects of stimulatory and inhibitory phosphorylation sites in the R domain. Am. J. Physiol. 1997; 273:L127–133. [PubMed: 9252549]
14. Pyle LC, Ehrhardt A, Mitchell LH, Fan L, Ren A, Naren AP, Li Y, Clancy JP, Bolger GB, Sorscher EJ, Rowe SM. Regulatory domain phosphorylation to distinguish the mechanistic basis underlying acute CFTR modulators. Am. J. Physiol. Lung Cell. Mol. Physiol. 2011; 301:L587–597. [PubMed: 21724857]
15. McClure M, DeLucas LJ, Wilson L, Ray M, Rowe SM, Wu X, Dai Q, Hong JS, Sorscher EJ, Kappes JC, Barnes S. Purification of CFTR for mass spectrometry analysis: identification of palmitoylation and other post-translational modifications. Protein Eng. Des. Sel. 2012; 25:7–14. [PubMed: 22119790]
16. Zhang MM, Tsou LK, Charron G, Raghavan AS, Hang HC. Tandem fluorescence imaging of dynamic S-acylation and protein turnover. Proc. Natl. Acad. Sci. U. S. A. 2010; 107:8627–8632. [PubMed: 20421494]
17. Resh MD. Palmitoylation of ligands, receptors, and intracellular signaling molecules. Sci. STKE. 2006; 2006:re14. [PubMed: 17077383]
18. Lin DT, Makino Y, Sharma K, Hayashi T, Neve R, Takamiya K, Huganir RL. Regulation of AMPA receptor extrasynaptic insertion by 4.1N, phosphorylation and palmitoylation. Nat. Neurosci. 2009; 12:879–887. [PubMed: 19503082]
19. Hayashi T, Rumbaugh G, Huganir RL. Differential regulation of AMPA receptor subunit trafficking by palmitoylation of two distinct sites. Neuron. 2005; 47:709–723. [PubMed: 16129400]

20. Abrami L, Kunz B, Iacovache I, van der Goot FG. Palmitoylation and ubiquitination regulate exit of the Wnt signaling protein LRP6 from the endoplasmic reticulum. Proc. Natl. Acad. Sci. U. S. A. 2008; 105:5384–5389. [PubMed: 18378904]
21. Tian L, Jeffries O, McClafferty H, Molyvdas A, Rowe IC, Saleem F, Chen L, Greaves J, Chamberlain LH, Knaus HG, Ruth P, Shipston MJ. Palmitoylation gates phosphorylation-dependent regulation of BK potassium channels. Proc. Natl. Acad. Sci. U. S. A. 2008; 105:21006–21011. [PubMed: 19098106]
22. Valdez-Taubas J, Pelham H. Swf1-dependent palmitoylation of the SNARE Tlg1 prevents its ubiquitination and degradation. EMBO J. 2005; 24:2524–2532. [PubMed: 15973437]
23. Qanbar R, Bouvier M. Role of palmitoylation/depalmitoylation reactions in G-protein-coupled receptor function. Pharmacol. Ther. 2003; 97:1–33. [PubMed: 12493533]
24. Chini B, Parenti M. G-protein-coupled receptors, cholesterol and palmitoylation: facts about fats. J. Mol. Endocrinol. 2009; 42:371–379. [PubMed: 19131499]
25. Levental I, Lingwood D, Grzybek M, Coskun U, Simons K. Palmitoylation regulates raft affinity for the majority of integral raft proteins. Proc. Natl. Acad. Sci. U. S. A. 2010; 107:22050–22054. [PubMed: 21131568]
26. Kinlough CL, McMahan RJ, Poland PA, Bruns JB, Harkleroad KL, Stremple RJ, Kashlan OB, Weixel KM, Weisz OA, Hughey RP. Recycling of MUC1 is dependent on its palmitoylation. J. Biol. Chem. 2006; 281:12112–12122. [PubMed: 16507569]
27. Mueller GM, Maarouf AB, Kinlough CL, Sheng N, Kashlan OB, Okumura S, Luthy S, Kleyman TR, Hughey RP. Cys palmitoylation of the beta subunit modulates gating of the epithelial sodium channel. J. Biol. Chem. 2010; 285:30453–30462. [PubMed: 20663869]
28. Singaraja RR, Kang MH, Vaid K, Sanders SS, Vilas GL, Arstikaitis P, Coutinho J, Drisdel RC, El-Husseini Ael D, Green WN, Berthiaume L, Hayden MR. Palmitoylation of ATP-binding cassette transporter A1 is essential for its trafficking and function. Circ. Res. 2009; 105:138–147. [PubMed: 19556522]
29. Greaves J, Lemonidis K, Gorleku OA, Cruchaga C, Grefen C, Chamberlain LH. Palmitoylation-induced aggregation of cysteine-string protein mutants that cause neuronal ceroid lipofuscinosis. J. Biol. Chem. 2012; 287:37330–37339. [PubMed: 22902780]
30. Rush DB, Leon RT, McCollum MH, Treu RW, Wei J. Palmitoylation and trafficking of GAD65 are impaired in a cellular model of Huntington's disease. Biochem. J. 2012; 442:39–48. [PubMed: 22103299]
31. Raymond FL, Tarpey PS, Edkins S, Tofts C, O'Meara S, Teague J, Butler A, Stevens C, Barthorpe S, Buck G, Cole J, Dicks E, Gray K, Halliday K, Hills K, Hinton J, Jones D, Menzies A, Perry J, Raine K, Shepherd R, Small A, Varian J, Widaa S, Mallya U, Moon J, Luo Y, Shaw M, Boyle J, Kerr B, Turner G, Quarrell O, Cole T, Easton DF, Wooster R, Bobrow M, Schwartz CE, Gecz J, Stratton MR, Futreal PA. Mutations in ZDHHC9, which encodes a palmitoyltransferase of NRAS and HRAS, cause X-linked mental retardation associated with a Marfanoid habitus. Am. J. Hum. Genet. 2007; 80:982–987. [PubMed: 17436253]
32. Kim SJ, Zhang Z, Sarkar C, Tsai PC, Lee YC, Dye L, Mukherjee AB. Palmitoyl protein thioesterase-1 deficiency impairs synaptic vesicle recycling at nerve terminals, contributing to neuropathology in humans and mice. J. Clin. Invest. 2008; 118:3075–3086. [PubMed: 18704195]
33. Xu J, Hedberg C, Dekker FJ, Li Q, Haigis KM, Hwang E, Waldmann H, Shannon K. Inhibiting the palmitoylation/depalmitoylation cycle selectively reduces the growth of hematopoietic cells expressing oncogenic Nras. Blood. 2012; 119:1032–1035. [PubMed: 22144181]
34. Kappes JC, Wu X, Wakefield JK. Production of trans-lentiviral vector with predictable safety. Methods Mol. Med. 2003; 76:449–465. [PubMed: 12526179]
35. Jennings BC, Nadolski MJ, Ling Y, Baker MB, Harrison ML, Deschenes RJ, Linder ME. 2-Bromopalmitate and 2-(20hydroxy-5-nitro-benzylidene)-benzo[b]thiophen-3-one inhibit DHHC-mediated palmitoylation in vitro. J. Lipid Res. 2009; 50:233–242. [PubMed: 18827284]
36. Draper JM, Smith CD. Palmitoyl acyltransferase assays and inhibitors (Review). Mol. Membr. Biol. 2009; 26:5–13. [PubMed: 19152182]
37. Charollais J, Van Der Goot FG. Palmitoylation of membrane proteins (Review). Mol. Membr. Biol. 2009; 26:55–66. [PubMed: 19085289]

38. Fukata M, Fukata Y, Adesnik H, Nicoll RA, Bredt DS. Identification of PSD-95 palmitoylating enzymes. Neuron. 2004; 44:987–996. [PubMed: 15603741]
39. Lu D, Sun HQ, Wang H, Barylko B, Fukata Y, Fukata M, Albanesi JP, Yin HL. Phosphatidylinositol 4-kinase IIalpha is palmitoylated by Golgi-localized palmitoyltransferases in cholesterol-dependent manner. J. Biol. Chem. 2012; 287:21856–21865. [PubMed: 22535966]
40. Tian L, McClafferty H, Knaus HG, Ruth P, Shipston MJ. Distinct acyl protein transferases and thioesterases control surface expression of calcium-activated potassium channels. J. Biol. Chem. 2012; 287:14718–14725. [PubMed: 22399288]
41. Chase JFA, Tubbs PK. Specific inhibition of mitochondrial fatty acid oxidation by 2-bromopalmitate and its co-enzyme A and carnitine esters. Biochem. J. 1972; 129:55–65. [PubMed: 4646779]
42. Resh MD. Use of analogs and inhibitors to study the functional significance of protein palmitoylation. Methods. 2006; 40:191–197. [PubMed: 17012032]
43. King SA, Sorscher EJ. R-domain interactions with distal regions of CFTR lead to phosphorylation and activation. Biochemistry. 2000; 39:9868–9875. [PubMed: 10933805]
44. Bates E, Miller S, Alexander M, Mazur M, Fortenberry JA, Bebok Z, Sorscher EJ, Rowe SM. Bioelectric effects of quinine on polarized airway epithelial cells. J. Cyst. Fibros. 2007; 6:351–359. [PubMed: 17329172]
45. Tsutsumi R, Fukata Y, Fukata M. Discovery of protein-palmitoylating enzymes. Pflugers Arch. 2008; 456:1199–1206. [PubMed: 18231805]
46. Mitchell DA, Vasudevan A, Linder ME, Deschenes RJ. Protein palmitoylation by a family of DHHC protein S-acyltransferases. J. Lipid Res. 2006; 47:1118–1127. [PubMed: 16582420]
47. Ohno Y, Kihara A, Sano T, Igarashi Y. Intracellular localization and tissue-specific distribution of human and yeast DHHC cysteine-rich domain-containing proteins. Biochim. Biophys. Acta. 2006; 1761:474–483. [PubMed: 16647879]
48. Greaves J, Salaun C, Fukata Y, Fukata M, Chamberlain LH. Palmitoylation and membrane interactions of the neuroprotective chaperone cysteine-string protein. J. Biol. Chem. 2008; 283:25014–25026. [PubMed: 18596047]
49. Fernandez-Hernando C, Fukata M, Bernatchez PN, Fukata Y, Lin MI, Bredt DS, Sessa WC. Identification of Golgi-localized acyl transferases that palmitoylate and regulate endothelial nitric oxide synthase. J. Cell. Biol. 2006; 174:369–377. [PubMed: 16864653]
50. Goodwin JS, Drake KR, Rogers C, Wright L, Lippincott-Schwartz J, Philips MR, Kenworthy AK. Depalmitoylated Ras traffics to and from the Golgi complex via a nonvesicular pathway. J. Cell. Biol. 2005; 170:261–272. [PubMed: 16027222]
51. Rathenberg J, Kittler JT, Moss SJ. Palmitoylation regulates the clustering and cell surface stability of GABAA receptors. Mol. Cell. Neurosci. 2004; 26:251–257. [PubMed: 15207850]
52. Lukacs GL, Mohamed A, Kartner N, Chang XB, Riordan JR, Grinstein S. Conformational maturation of CFTR but not its mutant counterpart (delta F508) occurs in the endoplasmic reticulum and requires ATP. EMBO J. 1994; 13:6076–6086. [PubMed: 7529176]
53. Gilbert A, Jadot M, Leontieva E, Wattiaux-De Coninck S, Wattiaux R. Delta F508 CFTR localizes in the endoplasmic reticulum-Golgi intermediate compartment in cystic fibrosis cells. Exp. Cell Res. 1998; 242:144–152. [PubMed: 9665812]
54. Fisher JT, Liu X, Yan Z, Luo M, Zhang Y, Zhou W, Lee BJ, Song Y, Guo C, Wang Y, Lukacs GL, Engelhardt JF. Comparative processing and function of human and ferret cystic fibrosis transmembrane conductance regulator. J. Biol. Chem. 2012; 287:21673–21685. [PubMed: 22570484]
55. Ostedgaard LS, Rogers CS, Dong Q, Randak CO, Vermeer DW, Rokhlina T, Karp PH, Welsh MJ. Processing and function of CFTR-DeltaF508 are species-dependent. Proc. Natl. Acad. Sci. U. S. A. 2007; 104:15370–15375. [PubMed: 17873061]
56. Kang R, Wan J, Arstikaitis P, Takahashi H, Huang K, Bailey AO, Thompson JX, Roth AF, Drisdel RC, Mastro R, Green WN, Yates JR 3rd, Davis NG, El-Husseini A. Neural palmitoyl-proteomics reveals dynamic synaptic palmitoylation. Nature. 2008; 456:904–909. [PubMed: 19092927]

57. Ivaldi C, Martin BR, Kieffer-Jaquinod S, Chapel A, Levade T, Garin J, Journet A. Proteomic analysis of S-acylated proteins in human B cells reveals palmitoylation of the immune regulators CD20 and CD23. PLoS One. 2012; 7:e37187. [PubMed: 22615937]

58. Marin EP, Derakhshan B, Lam TT, Davalos A, Sessa WC. Endothelial cell palmitoylproteomic identifies novel lipid-modified targets and potential substrates for protein acyl transferases. Circ. Res. 2012; 110:1336–1344. [PubMed: 22496122]

59. Dowal L, Yang W, Freeman MR, Steen H, Flaumenhaft R. Proteomic analysis of palmitoylated platelet proteins. Blood. 2011; 118:e62–73. [PubMed: 21813449]

60. Wan J, Roth AF, Bailey AO, Davis NG. Palmitoylated proteins: purification and identification. Nat. Protoc. 2007; 2:1573–1584. [PubMed: 17585299]

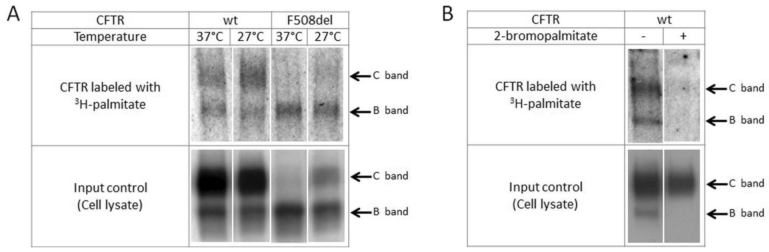

Figure 1. Palmitoylation of wild-type and F508del CFTR

(**A**) HEK293 cells transiently expressing CFTR were metabolically labeled with ^{3}H-palmitic acid. Subsequent immunoprecipitation of CFTR indicated that both wild-type and F508del CFTR are palmitoylated (top panel). As a control, 2% of cell lysate was reserved for analysis by western blot prior to IP (lower panel). (**B**) Treatment with the palmitoylation inhibitor 2-BP (100 μM during labeling – 4 h) in stably transduced HeLa wild-type cells inhibits labeling of CFTR as indicated by ^{3}H-palmitic acid (top panel). Cell lysate (2%) was studied by western blot prior to IP (lower panel).

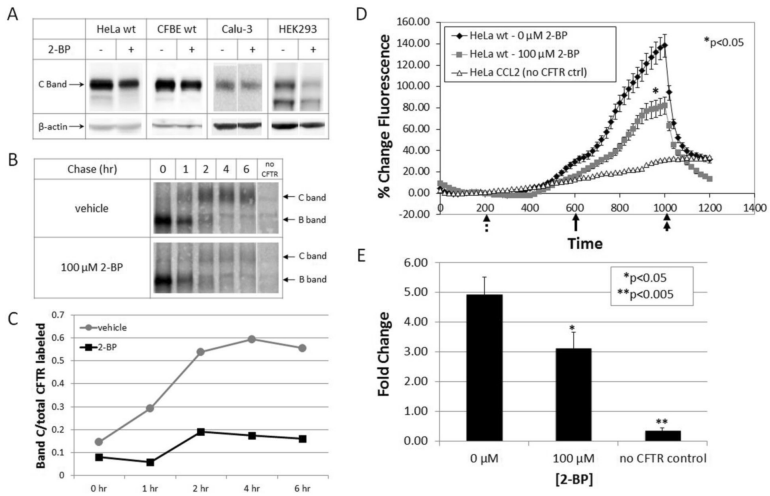

Figure 2. Influence of palmitoylation on maturation of wild-type CFTR

(**A**) Western blot using HeLa cells stably transduced to express wild-type CFTR, CFBE (cystic fibrosis bronchial epithelial cells) stably expressing wild-type CFTR, Calu-3 (airway serous glandular) cells with high level CFTR under regulatory control of the endogenous promoter, and HEK293 cells encoding doxycycline-inducible CFTR in presence or absence of 2-BP (100–150 μM, 8 h). CFTR steady state levels decreased when palmitoylation was inhibited. (**B**) Pulse-chase analysis of HEK293 cells (expressing wild-type CFTR) labeled with ^{35}S methionine and cysteine followed by a chase in the presence or absence of 150 μM 2-BP. Treatment with 2-BP prevents proper CFTR maturation as shown by failure of band B progression to band C. Results were quantified (**C**) as a ratio of radiolabeled band C at each time point to starting levels of total (labeled bands B + C) CFTR immediately following the pulse. Halide efflux was measured (**D**) and quantified (**E**) by the SPQ fluorescence assay. Forskolin (20 μM) and genistein (50 μM) were added (solid arrow) to stimulate CFTR-dependent ion transport (rate of upward deflection tracks CFTR activity). The findings indicate a decrease in CFTR activity when palmitoylation is inhibited. Dotted arrow = addition of dequenching buffer; double arrow = addition of quenching buffer. Results are shown as mean ± SEM and normalized to control cells. **P* < 0.05, ***P* < 0.005; *n* = 4.

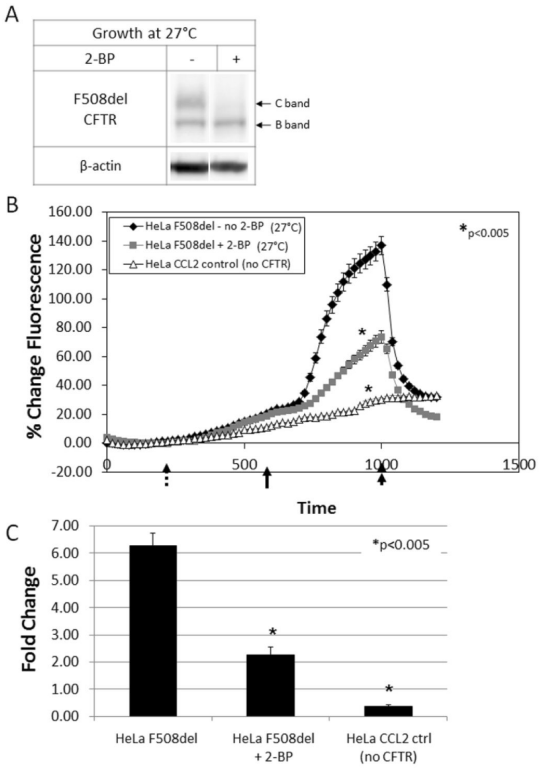

Figure 3. Influence of palmitoylation on low temperature correction of F508del CFTR

(**A**) Western blot of F508del CFTR grown at low temperature (27°C). Treatment with 2-BP led to diminished correction of F508del CFTR as indicated by the absence of band C. Halide efflux was measured (**B**) and quantified (**C**) by the SPQ fluorescence assay. Forskolin (20 μM) and genistein (50 μM) were added (solid arrow) to stimulate CFTR-dependent ion transport. The findings indicate a decrease in surface activity of low temperature corrected F508del CFTR when palmitoylation is inhibited by 2-BP. Dotted arrow = addition of dequenching buffer; double arrow = addition of quenching buffer. Results are shown as mean ± SEM and normalized to control cells. **P* < 0.005; *n* = 3.

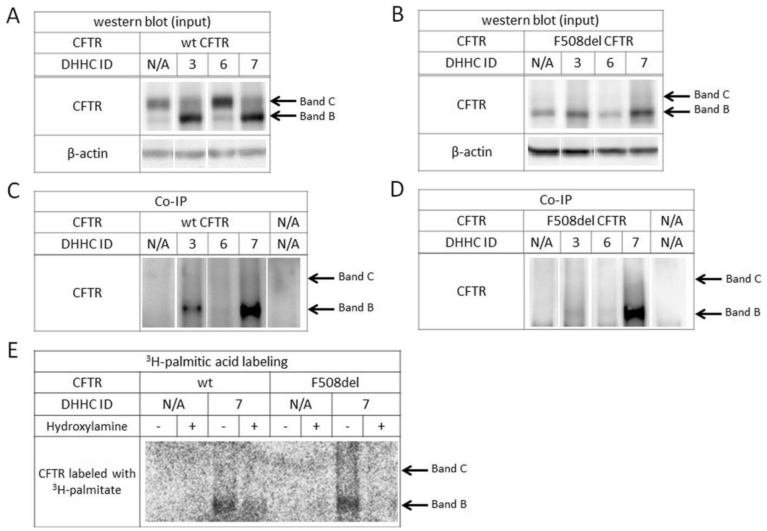

Figure 4. Contribution of protein acyl transferases to CFTR biogenesis

Western blot of HEK293 cells co-transfected with HA-tagged DHHC proteins and either wild-type (**A**) or F508del (**B**) CFTR indicate an increase in band B following overexpression of DHHC-7. Co-immunoprecipitation (DHHC proteins used as anchor) identified a robust interaction between DHHC-7 and wild-type CFTR (**C**) as well as F508del CFTR (**D**). Metabolic labeling with ^{3}H-palmitic acid in the presence of DHHC-7 resulted in enhanced CFTR palmitoylation (**E**), indicated by labeling after a 3–4 week exposure as compared to the 3–4 months required for CFTR labeling without DHHC-7. To verify palmitoylation, post-IP samples were split and treated with 1 M Tris-Cl (control) or 1 M hydroxylamine (pH 7.4) to remove palmitate via cleavage of the thioester bond.

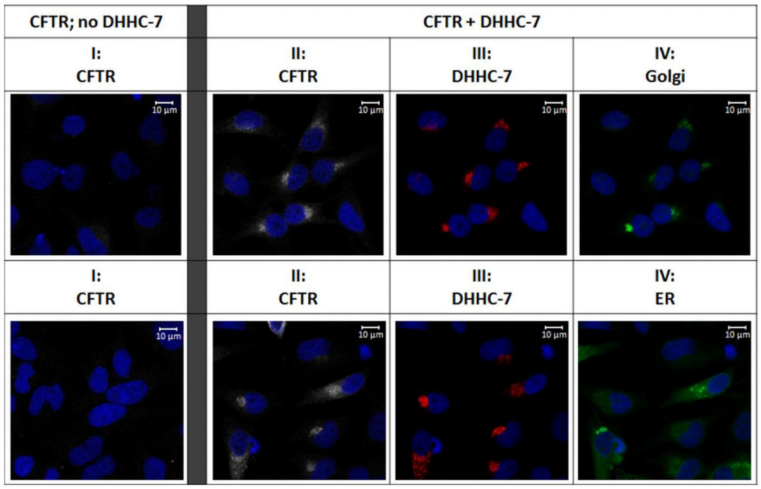

Figure 5. Immunofluorescence of HeLa F508del cells in the presence or absence of DHHC-7

F508del CFTR was labeled in the absence (column I) and presence (columns II–IV) of overexpressed DHHC-7. Mutant CFTR and HA-tagged DHHC-7 were labeled with anti-NBD1 and anti-HA antibodies, respectively. Golgi (top panel IV) or ER (lower panel IV) compartments were detected with CellLight GFP (Molecular Probes). Immunofluorescence identified strong co-localization of F508del CFTR with DHHC-7 and Golgi markers. The data also describe increased levels of F508del CFTR following overexpression of DHHC-7.